

Electrophysiological Properties of Rat Phrenic Motoneurons During Perinatal Development

MIGUEL MARTIN-CARABALLO AND JOHN J. GREER

Department of Physiology, Division of Neuroscience, University of Alberta, Edmonton, Alberta T6G 2S2 Canada

Martin-Caraballo, Miguel and John J. Greer. Electrophysiological properties of rat phrenic motoneurons during perinatal development. *J. Neurophysiol.* 81: 1365–1378, 1999. Past studies determined that there is a critical period at approximately embryonic day (E)17 during which phrenic motoneurons (PMNs) undergo a number of pivotal developmental events, including the inception of functional recruitment via synaptic drive from medullary respiratory centers, contact with spinal afferent terminals, the completion of diaphragm innervation, and a major transformation of PMN morphology. The objective of this study was to test the hypothesis that there would be a marked maturation of motoneuron electrophysiological properties occurring in conjunction with these developmental processes. PMN properties were measured via whole cell patch recordings with a cervical slice–phrenic nerve preparation isolated from perinatal rats. From E16 to postnatal day 1, there was a considerable transformation in a number of motoneuron properties, including 1) 10-mV increase in the hyperpolarization of the resting membrane potential, 2) threefold reduction in the input resistance, 3) 12-mV increase in amplitude and 50% decrease duration of action potential, 4) major changes in the shapes of potassium- and calcium-mediated afterpotentials, 5) decline in the prominence of calcium-dependent rebound depolarizations, and 6) increases in rheobase current and steady-state firing rates. Electrical coupling among PMNs was detected in 15–25% of recordings at all ages studied. Collectively, these data and those from parallel studies of PMN–diaphragm ontogeny describe how a multitude of regulatory mechanisms operate in concert during the embryonic development of a single mammalian neuromuscular system.

INTRODUCTION

Phrenic motoneurons (PMNs) and the diaphragmatic musculature are the major components of the respiratory neuromuscular system responsible for expanding the rib cage during inspiration. Relative to other neuromuscular systems, the PMN and diaphragm functional properties have to be in an advanced state of maturation by birth to ensure viability of the newborn. In fact, the PMN–diaphragm system is operational before birth to generate fetal breathing movements in utero (Jansen and Chernick 1991). It is known that the expansions of the rib cage associated with fetal breathing movements in utero are essential for proper lung maturation (Harding et al. 1993; Kitterman 1996). There was further speculation that central respiratory drive influences the maturation of the fetal respiratory neuromuscular system (Jansen and Chernick 1991). However, to critically test this hypothesis, a fundamental understanding of respiratory motoneuronal and muscle properties and their on-

togenesis during the perinatal period will be necessary. Toward this goal, the data outlined in this paper represent the initial contribution toward examining the correlation among PMN electrophysiological properties, the inception of fetal respiratory drive, and the onset of continuous rhythmic breathing at birth.

Previous studies using the perinatal rat model identified several key stages of phrenic nerve–diaphragm development (gestational period is 21 days; Fig. 1A). Phrenic axons emerge from the spinal cord at embryonic day (E) 11, migrate to contact the primordial diaphragm musculature by E13, begin to form intramuscular branches concomitantly with the initial formation of diaphragm myotubes at E14, and branch within the full extent of the developing diaphragm by E17–E18 (Allan and Greer 1997a). PMNs first receive descending inspiratory drive transmission and synaptic contacts from spinal afferents at E17 (Allan and Greer 1997b; Greer et al. 1992). Interestingly, the time of target innervation and the inception of functional recruitment coincide with the onset of a rapid and profound morphological development of PMNs (Allan and Greer 1997b). Thus, for the purpose of this study, we chose to examine the electrophysiological properties of PMNs during the critical period prior and subsequent to the major morphological reorganization, the completion of target musculature innervation, the onset of afferent and descending respiratory synaptic drive in utero, and continuous rhythmic activation at birth. To test the hypothesis that there would be a significant maturation of passive membrane properties, action potential characteristics, and repetitive firing properties of PMNs during this period, whole cell patch recordings of identified PMNs were performed with a cervical slice–phrenic nerve preparation isolated from perinatal rats ages E16, E18, and postnatal day (P) 0–1.

Regarding the general issue of the ontogeny of motoneuron electrophysiological properties, a number of experimental models was used in the past, including cultured preparations of dissociated chick motoneurons (McCobb et al. 1989, 1990), rat spinal explants (Xie and Ziskind-Conhaim 1995), and acutely isolated spinal cord segments (Di Pasquale et al. 1996; Fulton and Walton 1986; Ziskind-Conhaim 1988). Those studies provided valuable data demonstrating that, as motoneurons develop, there are typically changes in the action potential shape, firing patterns, and ionic conductances. This study of PMN development complements the past work by providing two important advantages. First, we are restricting our recordings to one class of target-specific mammalian motoneurons rather than pooling data from mixed populations within a given

The costs of publication of this article were defrayed in part by the payment of page charges. The article must therefore be hereby marked “advertisement” in accordance with 18 U.S.C. Section 1734 solely to indicate this fact.

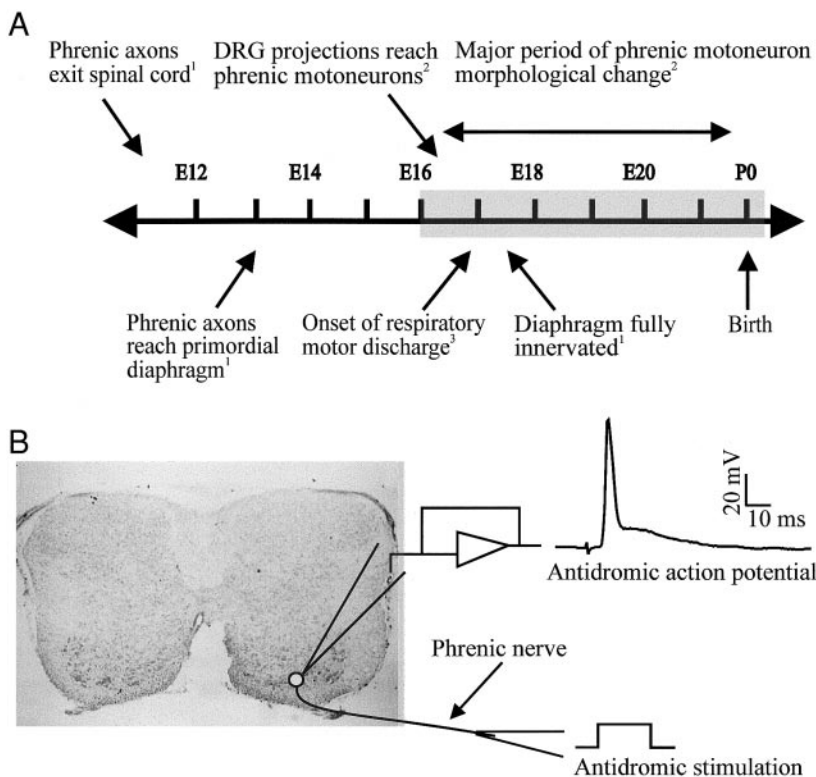


FIG. 1. A: time line indicating some of the key events involved in phrenic motoneuron (PMN)–diaphragm development. The shaded area [embryonic day (E)16 through P0–P1] represents the period in which electrophysiological properties were studied (Allan and Greer 1997a,b; Greer et al. 1992). B: schematic of experimental setup. Whole cell recordings were obtained from PMNs located in the ventromedial cervical spinal cord (shaded circle) in acutely isolated slice preparations. The phrenic nerve extending distal to the ventral root was left attached for identification of PMNs via antidromic stimulation.

ventral horn region. We are analyzing a population consisting of ~220 motoneurons that innervate one muscle. In contrast, when examining the development of mixed populations within cervical or lumbar ventral horns, one must contend with thousands of functionally heterogeneous motoneurons that innervate multiple muscles and develop at differing rates (Landmesser 1992). Second, we are taking the perspective of examining changes in PMN electrophysiological properties with respect to the overall context of our past findings regarding phrenic nerve–diaphragm development such as axon outgrowth, target innervation, functional recruitment, and morphological changes. Information regarding these aspects was not available in past studies of motoneuron development.

A preliminary account of this work appeared previously in abstracts (Martin-Caraballo and Greer 1997a,b).

METHODS

Cervical slice–phrenic nerve preparation

Embryos (E16–E18) were delivered from timed-pregnant Sprague-Dawley rats anesthetized with halothane (1.2–1.5% delivered in 95% O₂–5% CO₂) and maintained at 37°C by radiant heat, following procedures approved by the Animal Welfare Committee at the University of Alberta. To determine the timing of pregnancy, the day in which a morning test revealed the appearance of sperm plugs was designated E0. Fetal age was confirmed by comparing the crown–rump length of the embryos with previously published values by Angulo y Gonzalez (1932). Newborn rats (P0–P1) were anesthetized by inhalation of metofane. Embryos and newborns were decerebrated, and the brain stem–spinal cord with the phrenic nerve attached was dissected in artificial cerebrospinal fluid (CSF) equilibrated with 95% O₂–5% CO₂ (pH 7.4; 27 ± 1°C). A spinal segment was then cut from within the brain stem–spinal cord preparation with a vibratome

(Pelco; Redding, CA) into a single slice containing the C4 segment (E18, P0–P1) or C3–C4 segment (E16) with the phrenic nerve and the dorsal root ganglia attached (≈750 μm thick). The dorsal roots were then cut to prevent reflex-mediated synaptic stimulation of PMNs in response to antidromic stimulation of the phrenic nerve used for identification of PMNs. The spinal cord slice was transferred to a Sylgard-coated recording chamber and pinned down (at the dorsal border of the white matter) and continuously perfused with oxygenated artificial CSF solution at pH 7.4 and 27 ± 1°C (perfusion rate 2 ml/s, volume of the chamber 1.5 ml). The slice was left to equilibrate for at ≥1 h before recording, and data were typically acquired for ≤5 h after slice preparation. Previous measurements of O₂ tension within the tissue of similar *in vitro* preparations determined that neuronal populations are well oxygenated under these experimental conditions (Brockhaus et al. 1993; Jiang et al. 1991).

Whole cell recording

Recording electrodes were fabricated from thin-wall borosilicate glass (A-M Systems, Everett, WA). The pipette resistances were between 4 and 6 MΩ. To decrease capacitance transients, pipette tips were coated with Sigmacote (Sigma Chemical; St. Louis, MO), and the level of fluid submerging the slice was minimized during recordings. The electrode was advanced with a stepping motor (PMC 100, Newport; Irvine, CA) into the PMN pool located in the medial zone of the ventral horn close to the border between the white and gray matter. To avoid clogging of the recording electrode, positive pressure (≈30 mmHg) was applied while entering the tissue to a depth of ≥100 μm from the slice surface. Pressure was then removed while advancing within the PMN pool. Once the pipette made contact with a cell, negative pressure was used to form a gigaohm (>1 GΩ) cell–pipette seal, and gentle suction was then applied to rupture the patch membrane. Seal formation and membrane breakthrough were monitored by observing the response to hyperpolarizing current steps (0.3 nA). Whole cell recordings were initially established in the

artificial CSF solution and performed with an AxoClamp 2B amplifier (Axon Instruments; Foster City, CA). Liquid junction potentials were corrected before seal formation with the compensation circuitry of the patch-clamp amplifier. Data were filtered at 30 kHz, digitized via an A/D interface, and analyzed with pClamp (Axon Instruments) and Origin (Northampton, MA) software.

Seal formation and whole cell recordings were carried out in current-clamp mode. Once the whole cell configuration was established motoneurons were identified as belonging to the PMN pool by antidromic stimulation of the phrenic nerve via a suction electrode. Rectangular pulses of 0.5-ms duration and 0.5-Hz frequency were delivered with a pulse generator (Master 8, AMPI; Jerusalem, Israel), and pulse amplitude was manually controlled with a stimulus isolation unit (Iso-Flex, AMPI). Stimulation amplitudes for the phrenic suction electrode were ≤ 0.2 mA. To minimize current spread, the ground wire for antidromic stimulation was wrapped around the tip of the suction electrode. Antidromic action potentials were recorded on tape with a videocassette recorder (Sony, Tokyo) or captured with pClamp software for subsequent analysis. Neurons not responding to antidromic stimulation were not analyzed. Presumptive glial cells, characterized by having resting membrane potentials hyperpolarized beyond -70 mV and incapable of firing action potentials in response to antidromic or orthodromic stimulation, were also encountered but not analyzed.

Electrophysiological properties of PMNs were typically recorded at -60 mV holding membrane potential. However, the effects of differential holding membrane potentials on spike and firing properties were investigated by continuous injection of hyperpolarizing or depolarizing current as required. Independent action potentials were evoked by antidromic stimulation of the phrenic nerve or by intracellular injection of depolarizing current in the form of a 0.5-ms rectangular pulse. Repetitive firing properties were investigated after injections of 1 s-long depolarizing pulses of varying amplitudes. A schematic illustration of the slice preparation and electrode positioning is shown in Fig. 1B.

Resting membrane potential was determined immediately after breaking the seal between the membrane and the pipette. Action potential duration was measured at half-maximal amplitude. Input resistance (R_{in}) was determined from the voltage deflection on injection of a series of 400 ms-long hyperpolarizing current pulses (≤ 0.05 nA). The membrane time constant (τ) was calculated by fitting the membrane voltage response to injection of negative current. The membrane response could be closely fit by a single exponential. Threshold potential (V_{th}) was determined as the absolute membrane potential at the onset of an action potential. The mean rheobase (I_{th}) was calculated as the depolarizing voltage required to elicit an action potential (V_{th}) divided by its input resistance, assuming an ohmic membrane (DiPasquale et al. 1996). The duration of the afterhyperpolarization (AHP) was measured from the falling phase of the action potential to the point in the AHP membrane potential trajectory that returned to the holding membrane potential. The AHP amplitude was measured at the point of maximum voltage deflection relative to the holding membrane potential. Sag depolarization and rebound excitation were examined after injection of hyperpolarizing currents of increasing amplitudes. All data values are presented as means \pm SE. Significant differences between values before and after a drug treatment within a given age were calculated by using paired Student's *t*-test, whereas differences between various age groups were tested with analysis of variance (Origin).

Intracellular and extracellular solutions

Artificial CSF contained (in mM) 128 NaCl, 3 KCl, 0.5 NaHPO₄, 1.5 CaCl₂, 1 MgCl₂, 23.5 NaHCO₃, and 30 glucose (pH 7.4) when bubbling with 95% O₂-5% CO₂. In the calcium-free solution, calcium ions were replaced by an equimolar concentration of cadmium chlo-

ride, and NaHPO₄ was removed to avoid precipitation. The sodium-free solution (HEPES-based buffer) contained (in mM) 139 choline chloride, 10 HEPES, 3 KCl, 0.5 NaHPO₄, 1.5 CaCl₂, 1 MgCl₂, and 30 glucose (pH 7.4) with TrisOH and bubbled with 100% O₂. The standard pipette solution contained (in mM) 130 potassium gluconate, 10 NaCl, 1 CaCl, 10 1,2-bis(2-aminophenoxy)ethane-*N,N,N',N'*-tetraacetic acid (BAPTA), 10 HEPES, 5 Mg ATP, and 0.3 NaGTP (pH 7.3) with KOH. The composition of the pipette solution with a lower calcium buffer capacity was similar to that of the standard solution except for the following changes. BAPTA was decreased to 0.1 mM, calcium was not added, and potassium gluconate was increased to 155 mM.

The osmolarity of all the external solutions was kept between 320 and 325 mosm, and the osmolarity of the pipette solutions was ~ 315 mosm as measured with a freezing point osmometer (Advanced Instruments; Needham, MA).

Drugs

Stock solutions of drugs were prepared as $\times 100$ – $1,000$ concentrates. All drugs were added into the perfusate by switching to reservoirs containing the appropriate test solution. A waiting period of ≥ 5 min was used to allow for equilibrium before data were collected. TTX (Sigma; St. Louis, MO) and lidocaine *N*-ethyl bromide (QX 314) (RBI; Natick, MA) were used.

RESULTS

Electrical properties of PMNs were determined from neurons meeting the criteria of having a stable resting membrane potential more negative than -45 mV and action potential amplitudes of ≥ 50 mV. There are two points that should be taken into consideration when interpreting the results obtained with the cervical slice preparation. First, PMNs were recorded at a depth of 100–200 μ m from the surface of the slice, which meant that, although large portions of their dendritic trees were intact, the distal rostrocaudally projecting dendrites were typically severed. Second, the normal endogenous synaptic drive received *in vivo*, which could influence PMN properties and behavior, will obviously be absent in our experimental conditions.

Membrane properties

Passive properties of developing motoneurons, in particular the resting membrane potential, firing threshold, and input resistance, are important factors in determining electrical excitability in response to synaptic inputs. Thus the first component of our study was to characterize age-related changes in PMN passive properties. Results from the population data are summarized in Table 1.

Between ages E16 and E18, approximately the time of the inception of inspiratory drive transmission, the resting membrane potentials became hyperpolarized by ~ 8 mV. Between E18 and birth there was a slight further hyperpolarization of ~ 2 mV in the resting membrane potential. Despite these changes in the resting membrane potential, the threshold for generating an action potential did not change substantially at any age studied. An $\sim 32\%$ reduction in the input resistance occurred between E16 and E18. A further $\sim 48\%$ decrement in input resistance occurred by birth. With no significant variation in threshold potential, the threefold increase in the mean rheobase from E16 to P0–P1 was most likely due to the reduction

TABLE 1. *Electrophysiological properties of PMNs*

	E16	E18	P0-P1
Action potential amplitude, mV	66.5 ± 2.0	68.1 ± 1.6	78.3 ± 2.5*
Action potential duration, ms†	6.2 ± 0.5	4.1 ± 0.3‡	3.2 ± 0.2‡§
Resting membrane potential, mV	-49.3 ± 5.9	-57.4 ± 2.0	-59.3 ± 1.2*
Input resistance, MΩ ^a	806 ± 81	551 ± 61*	266 ± 33‡§
Mean rheobase, pA ^b	35 ± 4	42 ± 6	89 ± 14‡§
Time constant, ms ^c	53.0 ± 4.6	46.0 ± 5.0	38.0 ± 3‡

† Action potential duration at half-maximal amplitude; * $P \leq 0.05$; ‡ $P \leq 0.01$ vs. E16; § $P \leq 0.05$ vs. E18. ^a Input resistance was calculated from the voltage responses to injections of small hyperpolarizing current pulses (400 ms, 10–30 nA). ^b Mean rheobase was determined by dividing the threshold potential by input resistance. ^c Time constant was obtained by fitting the voltage transient induced by the injection of hyperpolarizing current to an exponential function.

in the input resistance of PMNs. An analysis of the voltage responses to hyperpolarizing currents (Fig. 2) also revealed that the membrane time constants of PMNs were significantly reduced (by ~29%) during the transition from E16 to P0–P1 (Table 1).

Subthreshold membrane responses to hyperpolarizing current injections were studied to assess whether there were age-related changes in inward rectification and rebound depolarization (Bayliss et al. 1994; Dekin and Getting 1987). The voltage deflections of membrane potentials after injections of prolonged hyperpolarizing current pulses (400 ms) are shown in Fig. 2A. Plots of the voltage responses at the onset (V_{initial}) and end ($V_{\text{steady state}}$) of the current pulses resulted in superim-

posed linear graphs (Fig. 2B), indicating the lack of sag depolarization and inward rectification at all ages examined. The level of inward rectification was also determined as the percentage ratio of $V_{\text{steady state}}/V_{\text{initial}}$ at -100 ± 10 mV membrane potential. The values obtained were similar at all ages [E16, $99 \pm 0.4\%$ ($n = 18$); E18, $99 \pm 0.3\%$ ($n = 16$); P0–P1, $100 \pm 0.1\%$ ($n = 10$)].

Rebound depolarizations after the completion of hyperpolarizing current pulses were observed in a subpopulation of PMNs, with the presence decreasing with age. Approximately 65% of E16 PMNs exhibited rebound depolarizations (11/17); this value decreased to 45% in E18 (5/11) and to 12% in P0–P1 (3/26) PMNs. As the strength of the hyperpolarizing pulse was increased, the depolarizing rebound potential eventually reached threshold, triggering an action potential (Fig. 2A). Rebound depolarizations were not inhibited in the presence of the intracellular sodium channel blocker QX 314 (1.5 mM) (Connors and Prince 1982) or after blockade of potassium channels with intracellular TEA and cesium ions (Fig. 3C). Incubation of the spinal slice in a calcium-free solution eliminated the rebound depolarizations, thus indicating that a calcium-mediated conductance generates the rebound depolarizations (Fig. 3A). As also shown in Fig. 3, activation of the rebound depolarization was dependent on the amplitude (B) and duration (C) of the hyperpolarizing potential. Hyperpolarizations greater than -75 mV and duration of ≥ 200 ms were required for the expression of rebound depolarization. Further increases in the strength and duration of the hyperpolarizing stimulation were followed by larger depolarizing responses.

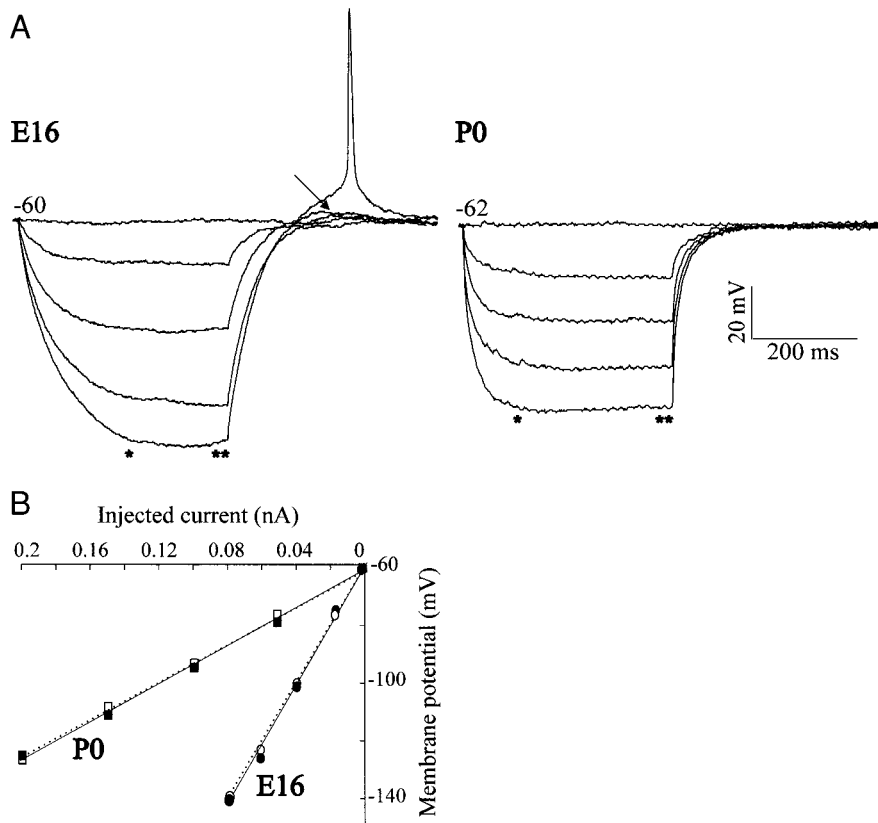


FIG. 2. Membrane responses to the injection of hyperpolarizing current pulse revealed the presence of a rebound excitation (arrow) in E16 PMNs and the lack of sag depolarization at all ages examined. A: membrane voltage responses of E16 and P0 PMNs after injection of 400 ms-long hyperpolarizing current pulses of increasing amplitude. At E16 rebound excitation followed the end of the hyperpolarizing pulse (arrow). An action potential was evoked by further increasing the strength of the current stimulation. * and **: points in which the membrane voltage response was measured for the I/V plots. B: plots of the injected current vs. membrane voltage responses for the PMNs shown in A (E16, square; P0, circle). Voltages were measured when the membrane response reached its maximum (discontinuous line; nonfilled points) and near the end (continuous line; filled points) of the pulse as indicated in A by * and **, respectively. The I/V plots resulted in superimposable linear graphs, indicating the lack of sag depolarization.

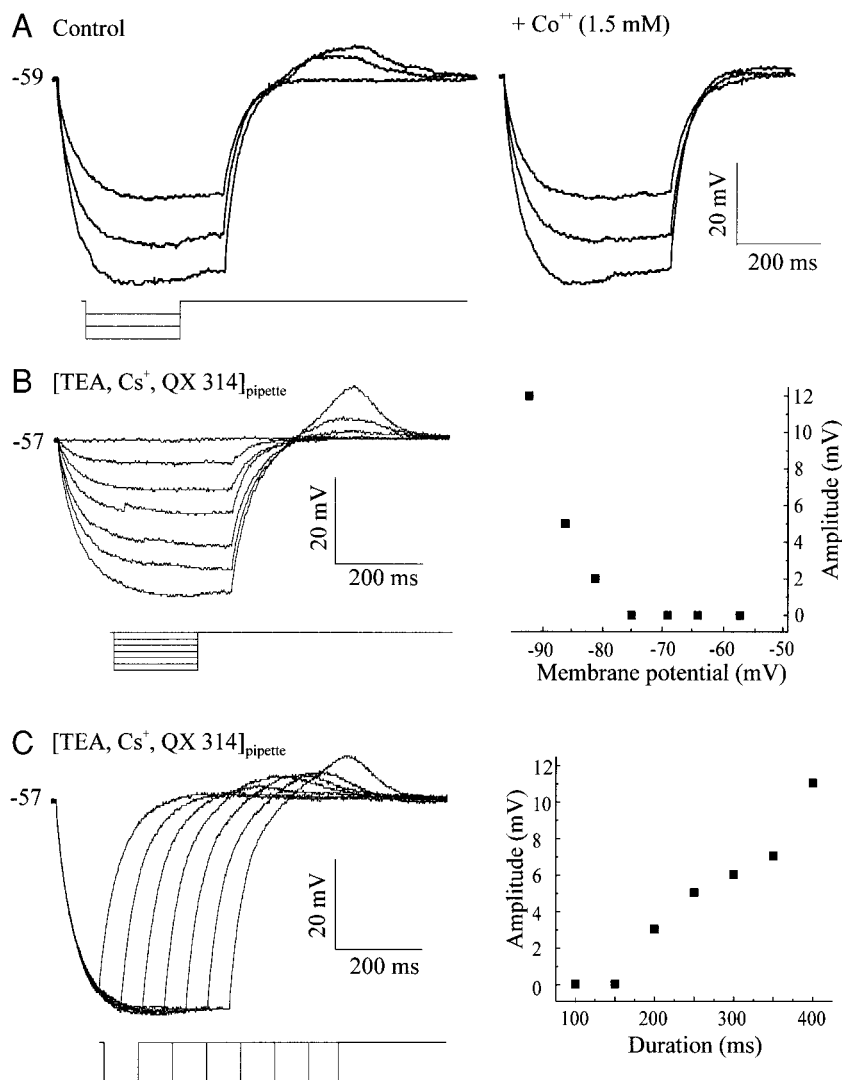


FIG. 3. Characterization of the rebound depolarizations observed in E16 PMNs. *A*: rebound depolarizations were calcium dependent. *Left panel*: control recording. *Right panel*: recording after calcium currents were blocked by the addition of cobalt ions to the bathing solution. In contrast, when calcium conductances are unperturbed and sodium and potassium conductances were blocked, the rebound depolarizations persisted (see traces *B* and *C*). *B*: rebound depolarization amplitude increased with increasing hyperpolarization. *Left*: rebound depolarization at different levels of hyperpolarization. *Right*: membrane potential-rebound depolarization amplitude plot for the cell response on the left. *C*: rebound depolarization amplitude increased with increasing duration of the hyperpolarizing pulse. *Left*: rebound depolarization at increasing duration of hyperpolarization. *Right*: magnitude of the rebound depolarization at increasing duration of hyperpolarization for the cell response on the left. Recordings shown in *B* and *C* were carried with a pipette solution containing QX 341 (1.5 mM) to block sodium-mediated conductance and TEA and cesium ions to block potassium-mediated conductances.

Action potential characteristics

Previous studies demonstrated that age-related changes in action potential parameters are often influenced by the holding membrane potential (McCobb et al. 1990; Spigelman et al. 1992). Thus age-dependent comparisons between PMNs were standardized by holding the membrane potential at approximately -60 mV at all ages, before investigations of the influence of depolarizing and hyperpolarizing holding potentials. From E16 to P0–P1, action potential amplitude increased by ~ 12 mV (Table 1). There was a particularly striking decrease of $\sim 34\%$ in the action potential duration pre- and postinception of the inspiratory drive transmission between E16 and E18 (Table 1). From E18 through to P0–P1, the action potential duration underwent a further $\sim 27\%$ decrease (Table 1).

The action potential spike was followed by afterpotentials of various shapes, depending on age (Fig. 4). At E16 the action potential spike was followed by a slowly decrementing afterdepolarization (ADP), with no clear indication of an AHP. Through ages E18 to P0–P1, a hump-like ADP and a medium-duration afterhyperpolarizing potential (mAHP) developed. Further, a fast AHP (fAHP) separated the repolarizing component of the spike from the following ADP in

a subpopulation of P0–P1 PMNs (Fig. 4). The fAHP was expressed as an early-peaking, brief duration potential, whereas the mAHP peaked later and had a more prolonged time course (≥ 50 ms; Fig. 4, P0).

A further analysis of the age-dependent changes in the expression of the mAHP was performed as a result of potential concerns with the standard pipette solutions used during our recordings. Previous results from a variety of neuronal recordings demonstrated that the mAHP is often due to the activation of a calcium-activated potassium conductance (Viana et al. 1993b; Walton and Fulton 1986). Our data showing that incubation of the neonatal spinal slice in calcium-free buffer (discussed in IONIC CONDUCTANCES UNDERLYING COMPONENTS OF ACTION POTENTIAL) resulted in the inhibition of the mAHP among neonatal PMNs supported this idea (Fig. 6C). However, we thought it possible that a significant component of the mAHP may have been blunted with our standard pipette solution, which contained 10 mM of the calcium chelator BAPTA (e.g., a small mAHP may have been present but obscured in E16 PMNs). Thus we repeated our recordings with a pipette solution with a lower calcium buffer capacity (reduced from 10 to 0.1 mM BAPTA; Fig. 5). The exact intracellular calcium

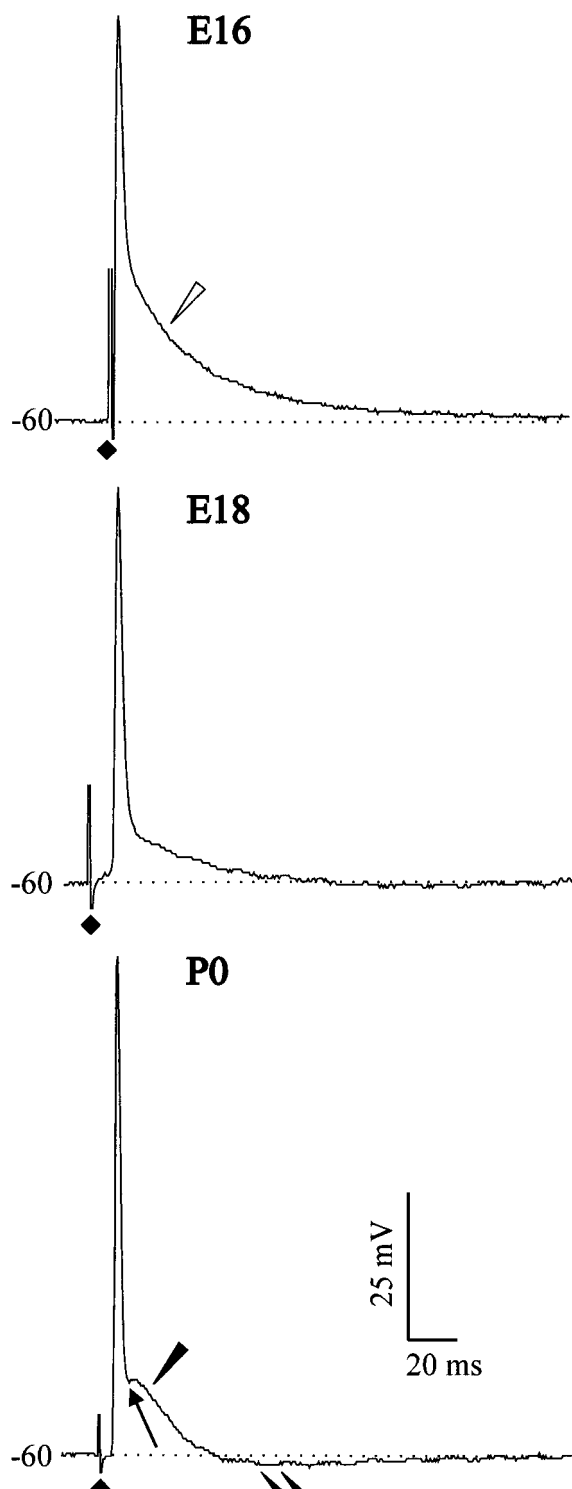


FIG. 4. Typical action potentials recorded from E16, E18, and P0 PMNs. Action potentials were evoked by antidromic stimulation of the phrenic nerve from a holding potential of approximately -60 mV. The stimulation artifact associated with antidromic stimulation is represented by a diamond in this and following figures. From E16 to P0, the action potential became shorter in duration and larger in amplitude. A slowly decaying afterdepolarization (ADP, empty arrowhead) is present at E16 but is replaced by a hump ADP (filled arrowhead) prominent in P0 PMNs. A medium-duration afterhyperpolarization (mAHP, double-filled arrowheads) and a fast AHP (long arrow) are present in neonatal PMNs.

concentrations reached during an action potential in the presence of the two levels of calcium chelation cannot be determined without direct measurements of the spatiotemporal distribution of calcium levels within the neuron during the course of an action potential. However, by using a software package designed to calculate the relative buffering capacities of whole cell patch solutions (Sol I. D.; E. A. Erter, Univ. of Washington) and taking into consideration what was estimated regarding calcium influx during an action potential (Jassar et al. 1994; Lockery and Spitzer 1992) we approximated the intracellular calcium concentrations that would be reached with the two solutions during an action potential. We estimated that in the presence of 1- to $50\text{-}\mu\text{M}$ range of calcium influx the calcium concentrations would range from 8.4 to 221.1 nM with the low BAPTA solutions compared with 24.3–25.3 nM with the standard solution. Thus we were confident that any calcium-mediated conductances would be amplified with the low BAPTA solution. However, even with the low BAPTA conditions, a mAHP was still not evident in any of the E16 PMNs recorded from ($n = 5$; Fig. 5). A mAHP was observed in 2 of 5 E18 PMNs in the modified low calcium-buffering solution compared with 5 of 19 PMNs in the standard solution. The amplitude (1.5 ± 0.4 vs. 2.5 ± 0.5 mV, $P \leq 0.05$) and duration (69 ± 8 vs. 93 ± 18 ms, $P \leq 0.05$) of the mAHPs in E18 PMNs also differed with the low intracellular calcium buffering. In P0–P1 PMNs, a clear mAHP was observed in all 5 PMNs tested with the modified low calcium-buffering solution compared with 8 of 30 PMNs in the standard recording solution. The amplitude (1.9 ± 0.4 vs. 4.6 ± 0.4 mV, $P \leq 0.05$) but not the duration (124 ± 20 vs. 117 ± 21 ms) of the mAHPs in P0–P1 PMNs differed under the modified conditions. It should be noted that, at all ages studied, the action potential amplitude tended to deteriorate (as much as 50%) within ~ 30 min after establishing the whole cell configuration when using the 0.1 mM BAPTA recording solution. Thus, although the low BAPTA solution was useful for delineating the presence and amplifying the effects of calcium-mediated conductances in the shaping of the action potential, it was not suitable for routine long-term stable recordings.

Figure 5 demonstrates that the amplitudes of the afterpotentials observed in PMNs at each age were dependent on the holding potential. In E16 PMNs, the slowly decaying ADP was enhanced with hyperpolarizing holding potentials. In P0–P1 PMNs, the hump-like ADP was also enhanced with hyperpolarizing holding potentials and diminished by depolarizing potentials. In contrast, the mAHPs observed in E18 and P0–P1 PMNs were enhanced by depolarizing holding potentials. Thus the repetitive firing frequencies and patterns, which are modulated by the afterpotential characteristics of the individual action potentials, will be influenced by the resting membrane potential.

Ionic conductances underlying the components of the action potential

IONIC DEPENDENCE OF ACTION POTENTIAL CHARACTERISTICS. A detailed analysis of the ionic conductances associated with age-dependent changes of the action potential characteristics is currently being analyzed with voltage-clamp techniques and is beyond the scope of this study. However, we did examine the

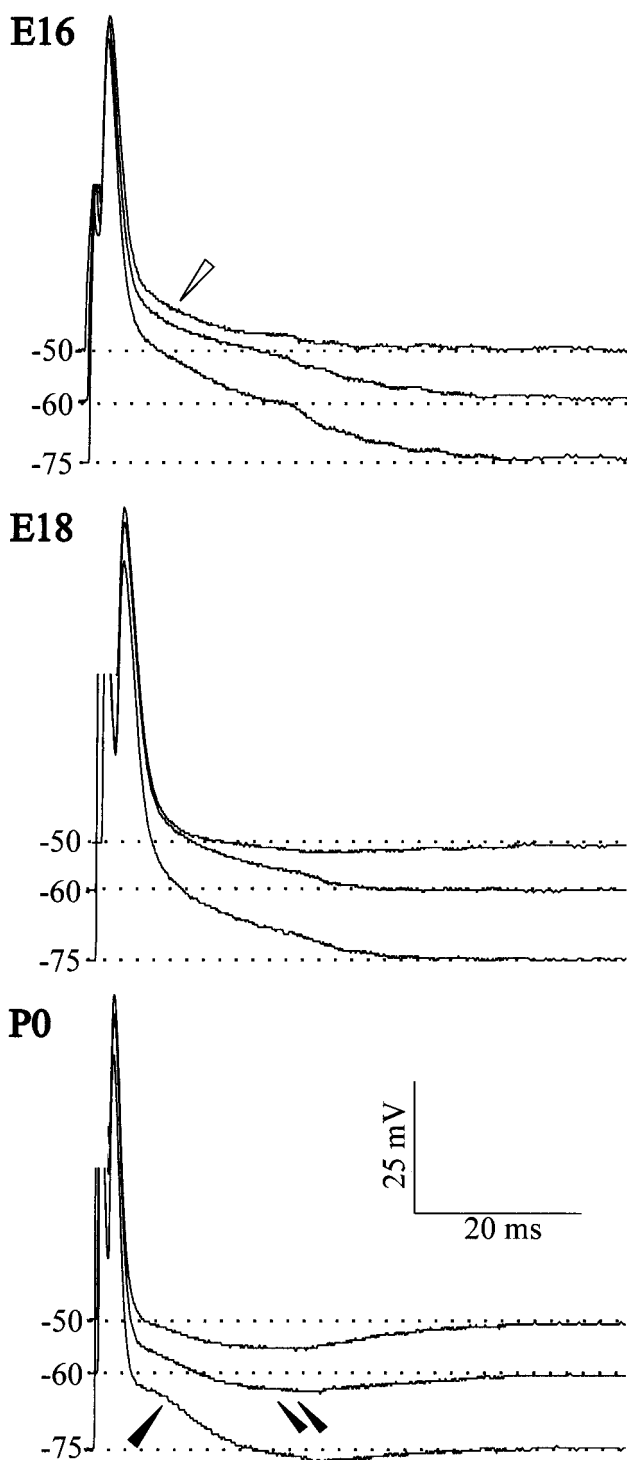


FIG. 5. The amplitudes of ADPs and AHPs were dependent on the membrane holding potential (held at -50 , 60 , and 75 mV). The slowly decrementing (empty arrowhead) and hump ADP (filled arrowhead) were enhanced by negative holding membrane potentials (approximately -75 mV), whereas the mAHP potential (double-filled arrowheads) was enhanced by more positive holding potentials (approximately -50 mV). Action potentials were evoked by 0.5 -ms intracellular current injection. Stimulation artifacts were truncated for clarity. These current-clamp recordings were carried out with the low 1,2-bis(2-aminophenoxy)ethane- N,N,N',N' -tetraacetic acid (0.1 mM) pipette solution to accentuate afterpolarizations influenced by intracellular calcium ions.

relative contributions of sodium and calcium currents in the generation of action potential characteristics (Spitzer and Baccaolini 1976; Ziskind-Conhaim 1988). As early as E16, the action potentials of PMNs were sodium dependent, as demonstrated by blocking sodium channels externally with TTX (0.5 – 1 μ M; $n = 5$; Fig. 6A). Incubation of the spinal slice in sodium-free buffer ($n = 4$) or addition of the intracellular blocker of sodium channels QX314 (1.5 mM, $n = 10$) to the pipette solution was also effective in preventing action potential generation in E16 PMNs (data not shown). A calcium component contributed to prolonging the duration of the action potential of E16 PMNs, as indicated by the reduction of the spike duration after incubation in a calcium-free buffer (Fig. 6B). The action potential duration of E16 PMNs decreased by $30 \pm 8\%$ ($n = 5$) in calcium-free buffer. However, in E18 PMNs, elimination of external calcium did not interfere significantly with spike duration. In four of seven P0–P1 PMNs, there was a slight increase of $15 \pm 6\%$ in spike duration after incubation in calcium-free buffer (Fig. 6C), suggesting that a calcium-dependent potassium current is involved in spike repolarization in neonatal PMNs. This idea was further supported by the fact that in P0–P1 PMNs the duration of the action potential was significantly lower when recorded with a modified low-BAPTA-pipette solution [2.0 ± 0.2 ($n = 6$) versus control high-BAPTA solution 3.2 ± 0.2 ms ($n = 26$), $P \leq 0.05$].

IONIC DEPENDENCE OF AFTERDEPOLARIZING POTENTIALS. Previous work indicated that ADPs observed in other motoneuronal populations are calcium dependent (Walton and Fulton 1986; Viana et al. 1993a). Thus we tested whether this applies to both the slowly decrementing and the hump-like ADPs observed in PMNs. As expected, both the slowly decrementing and hump ADPs were reduced by bathing the slice in a calcium-free solution (Fig. 6, B and C, respectively). We also considered whether the ADPs could be in part because of passive spreading of current through gap junctions. However, if this were the case, the amplitude of the ADPs would not have been voltage dependent (Walton and Navarrete 1991). As illustrated in Fig. 5, ADP amplitudes were enhanced at hyperpolarizing potentials and reduced at depolarizing potentials.

Electrotonic coupling among PMNs

Our initial intent was to use antidromic stimulation of the phrenic nerve to verify the identity of PMNs. However, rather unexpectedly, we noted that in a subpopulation of PMNs subthreshold antidromic stimulation of the phrenic nerve resulted in the generation of low-amplitude depolarizing potentials (Fig. 7A; observed in 3/22 E16, 5/19 E18, and 8/30 P0–P1 PMNs). This depolarizing potential had a very short latency with respect to the onset of the antidromic action potential, referred to as a short latency depolarization (SLD) (Walton and Navarrete 1991). In accordance with previous work (Walton and Navarrete 1991), the SLDs are indicative of electrotonic coupling among PMNs because of the presence of gap junctions. We classified SLDs as electrotonic if at least three of the following criteria were met: 1) depolarizing potentials had a short latency with respect to the antidromic action potential, 2) an increase in stimulation strength evoked a graded response of the SLD, 3) SLDs were resistant to high-frequency stimulation

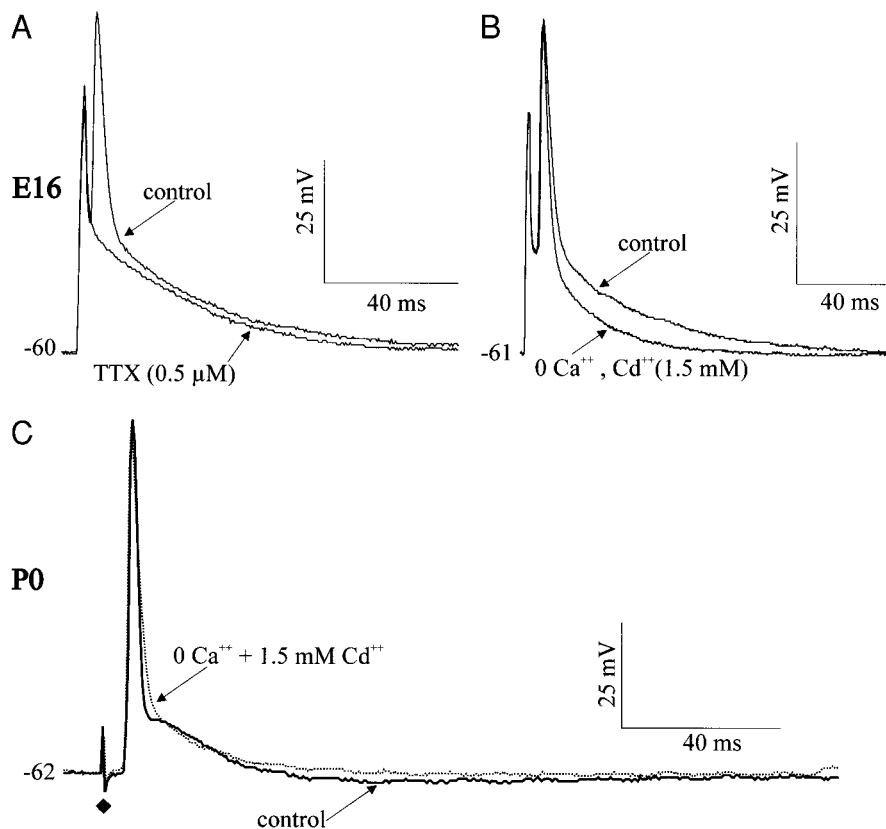


FIG. 6. Role of sodium and calcium conductance in the generation of action potentials. By age E16 the action potential is sodium dependent, and a calcium component contributes to prolonging the spike duration. In neonatal PMNs (P0), calcium is involved in the generation of afterpotentials and in repolarizing the action potential. *A*: action potential is dependent on activation of sodium channels by E16, as indicated by the abolition of spikes resulting from TTX ($0.5 \mu\text{M}$). *B*: incubation in calcium-free medium shortened the action potential duration and reduced the slowly decrementing ADP (E16). *C*: in neonatal PMNs, removal of external calcium prolonged the action potential duration and inhibited the mAHP and hump ADP.

(20 Hz), 4) SLDs were not affected by collision of an orthodromic action potential (generated by somatic current injection) with the antidromic spike, 5) SLDs were insensitive to holding potential, and 6) SLDs were unaffected by removal of external calcium or blockage of calcium conductances. It should be noted that reflex-mediated synaptic activity in the form of excitatory or inhibitory potentials (i.e., excitatory or inhibitory postsynaptic potentials) was not observed during recording of electrical activity of PMNs as the dorsal roots were cut. Further, no clear evidence for the presence of Renshaw neurons, in the form of high-frequency firing neurons, after antidromic stimulation was found (Hilaire et al. 1986).

As shown in Fig. 7A, subthreshold stimulation of a P0 PMN evoked low-amplitude depolarizations that closely followed the onset of the antidromic action potential. In the particular PMN presented in Fig. 7A, subthreshold stimulation evoked two SLDs of increasing amplitude, indicating the presence of coupling among three PMNs. Removal of external calcium to prevent synaptic release did not diminish the graded SLD (Fig. 7B). Collision experiments were carried out to clearly visualize the SLDs after eliminating the contribution of the antidromic action potential during the invasion of the soma. When a soma-generated action potential was elicited before antidromic stimulation, an SLD (Fig. 7C, continuous line) was evoked where the antidromic action potential would be expected (Fig. 7C, discontinuous line). Further, high-frequency stimulation of the phrenic nerve did not reduce the expression of the SLD, indicating further that this depolarization is independent of synaptic activity (Fig. 7D). When the pipette solution contained the intracellular inhibitor of sodium channels QX 314 the antidromic action potential was eliminated as expected

within a few minutes of membrane rupture. However, the SLD, which was insensitive to the holding membrane potential, persisted (Fig. 7E), suggesting that this potential does not involve synaptically mediated postsynaptic events or the activation of voltage-sensitive ionic conductances within the neuron being recorded from (i.e., SLD resulted from passive spread of current from coupled neuron).

The coupling among PMNs was also reflected in the relatively lower input impedance and higher mean rheobase measured in neurons where coupling was detected compared with those where it was not. For E18 PMNs the input impedances in PMNs with and without SLDs were 387 ± 108 ($n = 5$) versus 555 ± 61 ($n = 16$), and the mean rheobases were 76 ± 32 ($n = 5$) versus 42 ± 6 ($n = 16$). For P0–P1 PMNs the input impedances in PMNs with and without SLDs were 106 ± 14 ($n = 7$) versus 266 ± 33 ($n = 26$), and the mean rheobases were 259 ± 86 ($n = 7$) versus 89 ± 14 ($n = 26$). Only one of three E16 PMNs showing SLDs were recorded with an intracellular solution that did not contain QX-314, and thus insufficient numbers were available for a statistically meaningful comparison of passive properties among neurons with and without SLDs at that age.

Repetitive firing properties

Changes in the passive and action potential properties have a critical effect on the firing pattern of differentiating neurons. Thus we investigated age-dependent changes in the firing properties of PMNs by injection of 1 s-long depolarizing pulses of increasing strength. The population data illustrating age-dependent changes in firing properties are listed in Table 2. Repre-

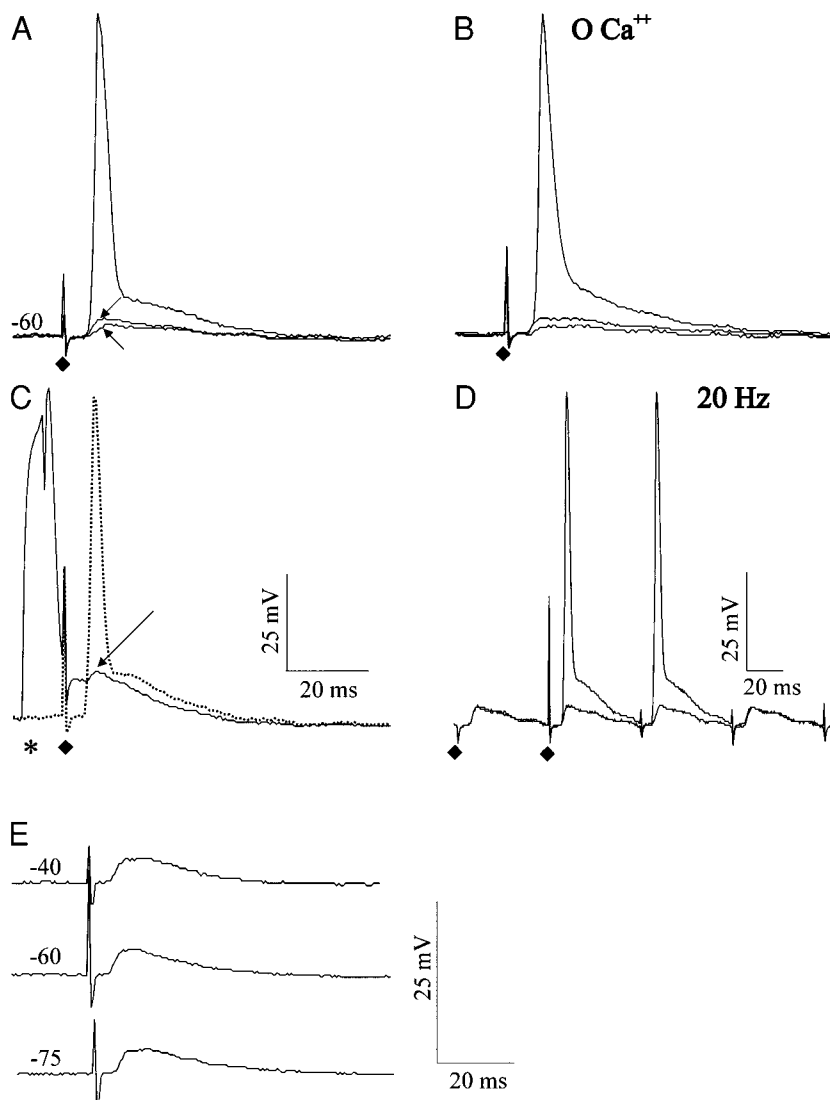


FIG. 7. Multiple criteria were used as evidence for electrical coupling among PMNs. *A*: low-amplitude, short latency depolarizations (SLDs) evoked by subthreshold antidromic stimulation of the phrenic nerve in a P0 slice. Subthreshold stimulations generated a graded response consisting of ≥ 2 SLDs (arrow). Increments in the stimulation intensity eventually induced an antidromic action potential. *B*: neither the antidromic spike nor the SLDs were eliminated by bathing in a calcium-free buffer. *C*: collision of a somatic action potential (generated by intracellular current injection, *) and an antidromic action potential (diamond) allowed for the observation of a low-amplitude depolarization (arrow) in place of the antidromic action potential (discontinuous line). The holding membrane potentials in *A–C* were -61 mV. *D*: high-frequency stimulation (20 Hz) of the phrenic nerve did not affect the low-amplitude SLDs. Two sweeps are represented in this figure; for clarity only the first antidromic artifact is represented by a diamond. An action potential was evoked after the fourth antidromic pulse. The measurements in *A–C* are from the same P0 motoneuron. *E*: in a different P0 motoneuron, low-amplitude SLDs were evoked with a pipette solution containing the intracellular blocker of sodium channels QX 314 (1.5 mM). Holding of membrane potential at various levels did not affect the amplitude of the electrotonic potentials.

representative data for PMNs of differing ages and firing characteristics are shown in Figs. 8 and 9. The majority of PMNs at all ages was able to generate sustained trains of action potentials with spike frequency adaptation (SFA) ($\sim 72\%$ of E16, 73% of E18, and 63% of P0–P1 PMNs; Fig. 8, *A–C*). At ages E16 and E18, however, $\sim 28\%$ of PMNs fired only one or a few action potentials during the 1 s-long depolarizing pulse (not shown). It is possible that these PMNs were damaged after electrode attachment or are among that population of PMNs that undergoes apoptosis during this period (Harris and McCaig 1984). However, these ideas are contradicted by the fact that the motoneurons had healthy membrane potentials, high-input impedances, and overshooting action potentials. Thus these embryonic PMNs with minimal firing capabilities may simply reflect a population with a relatively underdeveloped complement of ionic conductances. In P0–P1 PMNs, although the majority of neurons were able to generate continuous discharges with frequency adaptation, two further populations of PMNs with different firing patterns were observed. A second group of neonatal PMNs generated a burst of action potentials at the beginning of the depolarizing pulse (20%; Fig. 8*D*).

Bursting seemed to arise from an afterdepolarizing potential that followed the first spike. Bursting firing was enhanced by hyperpolarizing holding potentials (not shown). A third group of P0–P1 PMNs (17%) with a very low input resistance (113 ± 6 M Ω) required strong depolarizations (≥ 0.9 nA) to evoke firing (Fig. 8*E*). Of the seven PMNs within this group, SLDs indicative of electrical coupling were detected in five neurons. Thus the high-threshold and low-input impedance may be a direct result of coupling (Getting 1974; LoTurco and Kriegstein 1991). Although coupling was also observed among embryonic PMNs, the lack of a clear indication of a high-threshold population may have been due to the fact that the differences among PMN passive properties among those neurons with and without SLDs were not as exaggerated as was the case at P0–P1.

In E16 but not in older PMNs repetitive firing significantly altered the duration of the following spikes when compared with the first spike of the train (Fig. 8, *A* vs. *C* and *E*). Thus during repetitive firing in E16 PMNs action potentials became longer in duration, and their amplitude decreased over the first few intervals. Values for the duration of the first versus the last

TABLE 2. Changes in the firing properties of PMNs^a

	E16	E18	P0-P1
Firing threshold, I_{thr} , pA ^a	41 ± 5	48 ± 13	98 ± 18*‡
Firing frequency, Hz ^b			
I_{thr}	7.1 ± 0.5	9.8 ± 0.9	13.2 ± 0.7*‡
$2 \times I_{thr}$	14.4 ± 1.0	18.4 ± 1.3†	28.0 ± 2.3*‡
First ISI frequency, Hz			
I_{thr}	12.6 ± 0.9	13.9 ± 1.8	29.6 ± 3.7*‡
$2 \times I_{thr}$	24.1 ± 2.2	27.9 ± 2.6	52.5 ± 5.3*‡
Current–frequency slope, Hz/nA			
First ISI	444 ± 51	600 ± 75	501 ± 60
Last ISI	340 ± 43	327 ± 41	271 ± 44

Results were compiled from the firing discharges of PMNs that illustrate repetitive firing patterns similar to those in Fig. 8, A–C (i.e., bursting and high-threshold PMNs not included in data), after a series of 1-s depolarizing current pulses of increasing amplitude from a holding potential of approximately -60 mV. Measurements of the interspike intervals (ISIs) were carried out at the beginning and the end of the depolarizing pulse. ^aFiring threshold was determined as the lowest stimulation current necessary to evoke repetitive firing. ^bFiring frequency was determined as the number of action potentials per 1-s stimulation. ^cCurrent–frequency slope was the ratio of the first or last ISI frequency vs. injected current. (*) $P \leq 0.01$, (†) $P \leq 0.05$ vs. E16 or (‡) $P \leq 0.05$ vs. E18.

action potential in a 1 s-long train of spikes were as follows: E16 (6.4 ± 0.5 vs. 9.7 ± 1.3 , $n = 15$, $P < 0.05$); E18 (4.0 ± 0.2 vs. 4.3 ± 0.3 , $n = 14$); P0–P1 (3.7 ± 0.3 vs. 3.7 ± 0.4 , $n = 21$).

As revealed by the firing threshold (Table 2) and frequency–current plots (Fig. 8F), embryonic PMNs required lower levels of depolarizing current than neonatal PMNs to generate repetitive firing. The significant decrease in the input resistance of PMNs from E16 to P0–P1 meant that there was an age-dependent increase in the strength of the depolarizing current required to generate repetitive firing. For example, P0–P1 PMNs required an approximately twofold increase in the threshold current to evoke repetitive firing compared with E16 and E18 PMNs (Table 2). Among neonatal PMNs, the high-threshold motoneurons (likely electrotonically coupled neurons) required the highest levels of current stimulation to elicit repetitive firing (Fig. 8F).

Embryonic PMNs also tended to have a more limited firing range compared with neonatal PMNs (Fig. 8F, Table 2). The firing frequency during the 1 s-long stimulation pulse increased steadily between E16 and P0–P1 at the minimal level of depolarizing current required for repetitive firing and at twice that level (Table 2). The initial firing rate, i.e., the inverse of first interspike interval (ISI) duration, also increased steadily from E16 to P0–P1 as a function of the injected current (Table 2). The slope of the f–I plot for the first ISI did not change significantly among the age groups studied, although the slope of the last ISI decreased because of the decline in the firing rate with time (Table 2). SFA (Figs. 8 and 9) and a marked increase in the amount of SFA as a function of firing frequency (Fig. 9) were observed at all ages studied.

DISCUSSION

There are number of critical events associated with PMN development that occur at E17, including the inception of

functional recruitment via synaptic drive from medullary respiratory centers, arrival of spinal afferent terminals within the PMN pool, and the completion of intramuscular innervation of the diaphragm (Allan and Greer 1997a,b; Greer et al. 1992). During the ensuing 3- to 4-day period there is also a major transformation of PMN morphology (Allan and Greer 1997b) and the continuous rhythmic activation at birth. The current results demonstrate that PMNs undergo pronounced changes in their passive and active electrical properties in association with these developmental events.

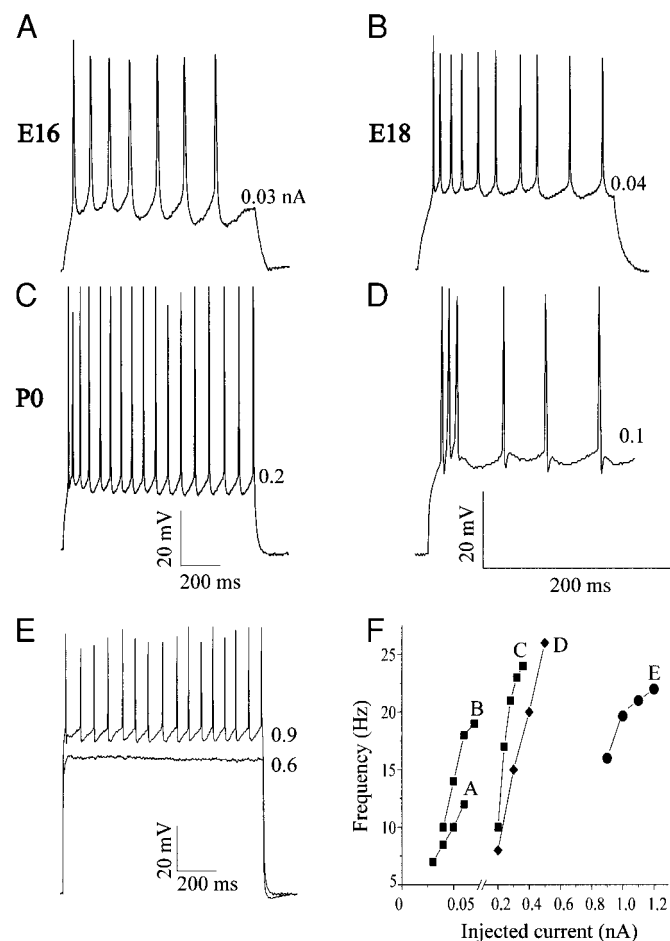


FIG. 8. Examples of repetitive firing patterns generated in E16, E18, and P0 PMNs after injection of 1-s depolarizing square pulse from a membrane holding potential of approximately -60 mV. The amplitudes of injected currents (nA) are shown beside each trace. The majority of E16 (A) and E18 (B) motoneurons exhibited a continuous firing discharge with adaptation. By P0, 3 distinct firing patterns developed among PMNs (C–E). The largest percentage of cells generated continuous firing with adaptation (C, 63%). In a smaller percentage of PMNs, firing was initiated by a rapid discharge of action potentials (D, 20%) or after injection of strong depolarizing currents (E, 17%), indicative of very low input resistance (i.e., high threshold). F: frequency–current plots for each of the neurons shown in traces A–E are shown in the frequency–current plot. Embryonic PMNs required significantly less current to reach firing threshold but had lower overall firing frequencies and current–frequency slopes than neonatal PMNs. Among neonatal PMNs, high-threshold neurons required significantly higher levels of current to obtain threshold and fired with a relatively high frequency of firing at threshold in comparison with lower-threshold PMN populations.

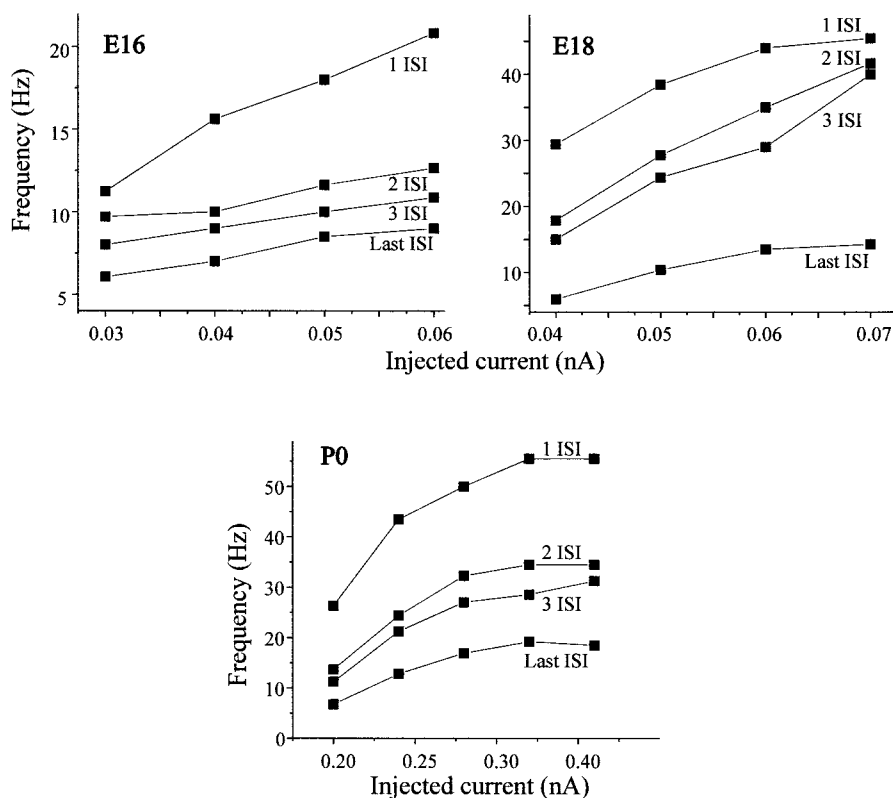


FIG. 9. Plots of the instantaneous firing rates for indicated interspike intervals as a function of injected current amplitude. Data are from neurons displaying continuous firing discharge patterns at ages E16, E18, and P0 shown in Fig. 8, A–C, respectively. At all ages studied, there was adaptation (i.e., the instantaneous firing frequency decreased during the course of the 1-s pulse) that was more pronounced at higher firing rates.

Development of membrane properties

During the period of PMN development spanning from E16 to P0–P1, the resting membrane potential becomes more hyperpolarized without a significant change in threshold, whereas the input resistance and time constant decreased. Thus PMNs are electrically more excitable at the inception of inspiratory drive (E17) compared with more mature states. Functionally, the increased propensity for firing will compensate for a relatively weak descending inspiratory drive from the medullary respiratory center and thus facilitate the production of fetal breathing movements (Di Pasquale et al. 1996; Greer et al. 1992). It was interesting to note that there was an ~ 8 mV change in the resting membrane potential of PMN spanning the 2-day period immediately before and postinception of inspiratory drive transmission (E16–E18). Future studies reexamining PMN electrophysiological properties at these ages when the descending drive transmission was experimentally eliminated will be useful for evaluating the relative importance of activity-dependent transformations of PMN resting properties.

This trend for changes in PMN passive properties is similar to that described during embryonic and postnatal development of spinal and brain stem motoneurons (Fulton and Walton 1986; Nunez-Abades et al. 1993; Viana et al. 1994; Xie and Ziskind-Conhaim 1995; Ziskind-Conhaim 1988) and hippocampal neurons (Spigelman et al. 1992). Further, a similar trend continues postnatally in PMNs (Cameron et al. 1990, 1991a,b). Several mechanisms could mediate the age-related changes in passive properties of motoneurons. A maturation in the relative permeability to sodium and potassium ions would

account for some of the hyperpolarizing of the resting membrane potential during PMN differentiation (Spigelman et al. 1992). Further, the regulation of the sodium-dependent chloride cotransporter is different in embryonic motoneurons, resulting in an increase in the intracellular concentration of chloride ions and a subsequent raising of the chloride equilibrium potential compared with more mature states (Rohrbough and Spitzer 1996; Wu et al. 1992). This idea is supported for PMNs by the fact that application of the classical inhibitory neurotransmitter GABA induces a depolarization of the neuronal membrane at E16 rather than a hyperpolarization typically observed in mature neurons (Martin-Caraballo and Greer, unpublished observations).

The reduction in the time constant and input resistance with age seems to reflect an increased density of ionic channels and cell size. An increase in the density of ionic conductances, as previously observed in developing chick motoneurons (McCobb et al. 1990), was suggested by the reduction of the membrane time constant and thus specific membrane resistance, ($R_{sp} = \tau_m/C_{sp}$, assuming no age-dependent changes in the specific membrane capacitance of $\sim 1 \mu\text{F}/\text{cm}^2$). Previous morphological studies demonstrated that PMNs undergo a significant increase in cell size and elaboration of the dendritic branching from E16 up to birth (Allan and Greer 1997b).

Presence of electrical coupling among perinatal PMNs

We detected the presence of electrical coupling among subpopulations of PMNs between ages E16 and P0–P1 (ranging from 14 to 26% of PMNs). The evidence to date suggests that at most two or three cells are coupled via gap junctions.

Previous findings from recordings of neonatal (P0–P3) rat thoracic motoneurons indicated coupling in as many 77% of lumbar motor neurons, with the mean number of cells per coupling being ~ 4.5 (Walton and Navarrete 1991). It may be that a similar degree of coupling is present in PMNs but at an earlier stage of development than we studied (i.e., pre-E16), as there is a clear rostrocaudal gradient of development within spinal neurons (Nornes and Das 1974). However, there are at least two reasons the presence of gap junctions may have been underestimated in our study. First, we only looked for SLDs that appeared subthreshold to the antidromic currents necessary to generate an antidromic action potential in the PMN being recorded from. Thus, in the event that the PMN being recorded from was coupled to a neuron with a higher threshold for antidromic activation (e.g., smaller-diameter axon), the coupling would remain undetected. Second, one cannot be assured that all axons within the nerve are stimulated by the suction electrode and/or conduct the antidromic action potentials to the full extent of the PMN pool.

Despite these limitations for quantifying the degree of electrical coupling, these are the first data demonstrating that there is in fact coupling among PMNs. Neuronal coupling among rat PMNs is clearly not present in the adult (Lipski 1984), and there is no evidence to date for dye coupling among postnatal PMNs ($>P1$) (Cameron, personal communication). We propose that the presence of neuronal coupling early in development and their removal with maturation would be functionally appropriate. The CNS utilizes two fundamental strategies for increasing the force produced by a muscle. First, the firing frequency of a given motor unit can be increased. Second, additional motor units can be recruited. In the case of fetal PMNs, at the inception of fetal respiratory movements, our data demonstrate that there are limits on the firing capabilities of PMNs. However, the presence of neuronal coupling facilitates the second strategy of increasing the number of motor units recruited for a given descending synaptic drive. Thus, although the descending drive may be relatively weak and the maximum discharge frequency of PMNs limited, the presence of coupling among the neuronal population will ensure adequate synchronous drive to the diaphragm for the purposes of generating perinatal breathing movements. As the animal matures, the situation changes to one where $<30\%$ of the PMN pool is recruited during an inspiratory effort at rest (Cameron et al. 1991; Torikai et al. 1996). Therefore it would be inappropriate and disadvantageous for neuronal coupling to persist among the PMN pool at a time when precise, graded recruitment is desired.

Development of action potential characteristics and associated ionic conductances

By E16, PMNs are capable of generating overshooting action potentials after intracellular injection of depolarizing current or antidromic stimulation. As observed during the embryonic (Di Pasquale et al. 1996; Spitzer and Baccaglini 1976) and postnatal (Fulton and Walton 1986; Viana et al. 1994; Ziskind-Conhaim 1988) maturation of other motoneurons, PMN action potentials increase in amplitude and decrease in duration between E16 and P0–P1. As demonstrated by McCobb et al. (1990), the increase in action potential amplitude during mo-

toneuron differentiation results from an increase in the density of voltage-gated sodium channels. The maturation of potassium conductances is important for spike repolarization and voltage-dependent changes in action potential duration in other neuronal systems (McCobb et al. 1990; Spigelman et al. 1992). Although voltage-clamp experiments are required to characterize the potassium conductances involved in shaping the action potential and firing properties of PMNs, the current findings suggest age-dependent changes in the expression of calcium-activated potassium conductances. First, removal of extracellular calcium contributes to prolonging the duration of action potential in neonatal PMNs only, whereas the use of a pipette solution with low calcium buffer capacity causes the opposite effect on action potential duration. This is consistent with the presence of a calcium-activated potassium conductance (likely of the maxi-type), which is involved in spike repolarization of neonatal motoneurons (Takahashi 1990; Viana et al. 1993b). Second, at E18, a calcium-dependent conductance generating the AHP (or small-type conductance) starts to develop and is fully expressed in the majority of neonatal PMNs. This conductance is prominent in neonatal motoneurons, where it plays a role in regulating repetitive firing frequencies and modulating SFA (Viana et al. 1993b; Walton and Fulton 1986).

We tested whether developing PMNs were capable of generating calcium-dependent action potentials, as was reported for developing amphibian spinal neurons (Spitzer and Baccaglini 1976). However, in PMNs, sodium ion influx is essential for action potential generation at the earliest ages studied (E16) and throughout further development. It remains to be determined whether calcium-mediated action potentials occur in PMNs at earlier ages ($\leq E15$). Nevertheless, whereas calcium spikes do not occur at E16, calcium ions do contribute significantly to prolonging the action potential at this age. The calcium-induced broadening of the action potential in PMNs is diminished rapidly after the inception of inspiratory drive transmission at E17 as no calcium component was seen to prolong the action potential spike at E18. There was also an age-dependent decrease in the presence of a calcium-dependent rebound depolarization, likely mediated by T-type conductances (Onimaru et al. 1996; Viana et al. 1993a), among PMNs. Functionally, beyond affecting firing properties, the influx of calcium ions is thought to be important for promoting neurite growth in developing neurons (Holliday and Spitzer 1990; Komuro and Rakic 1996; McCobb et al. 1989). This would be particularly important for PMNs during the period spanning E16–E19, when they undergo rapid growth and reorganization of axons and dendrites (Allan and Greer 1997b). Further, calcium fluctuations are important for regulating the maturation of voltage-gated ion channels during periods of electrophysiological maturation (Gu and Spitzer 1995).

Development of repetitive firing properties

The developmental changes of the passive properties and the ionic conductances shaping action potentials were responsible for a major change in the repetitive firing properties of PMNs. With the age-dependent reduction in the duration of individual action potentials, there was an increase in the overall repetitive

firing abilities of PMNs. Further, by P0, a second group of PMNs emerged that fired bursts of action potentials at the onset of a depolarizing pulse and may be related to early-recruited PMNs (Cameron et al. 1991b; Di Pasquale et al. 1996). A third group of PMNs required significantly stronger depolarizations to be activated. This likely reflected a group of PMNs that remained electrotonically coupled rather than the emergence of PMNs corresponding to high-threshold neurons observed at later stages of development (Cameron et al. 1991b; Di Pasquale et al. 1996). It will be interesting to examine the age-dependent changes in diaphragm contraction properties to see how they correlate with concomitant changes in PMN firing properties. Our preliminary observations indicate that the half-decay time of a single muscle twitch is two to three times longer at E18 compared with P0. Further, the minimum frequency of nerve stimulation necessary to achieve tetanus increases from a value of ~ 10 to 20 Hz from E18 to P0 (Martin-Caraballo and Greer, unpublished observations). Thus, although the action potential durations are longer and the firing frequencies are lower in embryonic PMNs compared with the neonate, the diaphragmatic contractile properties develop along a similar trend, allowing for tetanic contractions to occur at each developmental stage.

The authors thank Dr. W. E. Cameron for helpful comments. The free calcium concentration for the two solutions was estimated with software (Sol I. D.) written by E. A. Erter (Univ. of Washington, Seattle).

This work was funded by the Alberta Lung Association and the Medical Research Council of Canada. J. J. Greer is an Alberta Heritage Foundation for Medical Research (AHFMR) Senior Scholar and M. Martin-Caraballo was awarded an AHFMR Studentship.

Address for reprint requests: J. J. Greer, Dept. of Physiology, 513 HMRC, University of Alberta, Edmonton, Alberta T6G 2S2, Canada.

Received 15 July 1998; accepted in final form 6 November 1998.

REFERENCES

- ALLAN, D. W. AND GREER, J. J. Embryogenesis of the phrenic nerve and diaphragm in the fetal rat. *J. Comp. Neurol.* 382: 459–468, 1997a.
- ALLAN, D. W. AND GREER, J. J. Development of phrenic motoneuron morphology in the fetal rat. *J. Comp. Neurol.* 381: 469–479, 1997b.
- ANGULO Y GONZÁLEZ, A. W. The prenatal growth of the albino rat. *Anat. Rec.* 52: 117–138, 1932.
- BAYLISS, D. A., VIANA, F., BELLINGHAM, M. C., AND BERGER, A. J. Characteristics and postnatal development of a hyperpolarization-activated inward current in rat hypoglossal motoneurons in vitro. *J. Neurophysiol.* 71: 119–128, 1994.
- BROCKHAUS, J., BALLANYI, K., SMITH, J. C., AND RICHTER, D. W. Microenvironment of respiratory neurons in the in vitro brainstem-spinal cord of neonatal rats. *J. Physiol. (Lond.)* 462: 421–445, 1993.
- CAMERON, W. E., BROZANSKI, B. S., AND GUTHRIE, R. D. Postnatal development of phrenic motoneurons in the cat. *Dev. Brain Res.* 51: 142–145, 1990.
- CAMERON, W. E., HE, F., KALIPATNAPU, P., JODKOWSKI, J. S., AND GUTHRIE, R. D. Morphometric analysis of phrenic motoneurons in the cat during postnatal development. *J. Comp. Neurol.* 314: 763–776, 1991a.
- CAMERON, W. E., JODKOWSKI, J. S., FANG, H., AND GUTHRIE, R. D. Electrophysiological properties of developing phrenic motoneurons in the cat. *J. Neurophysiol.* 65: 671–679, 1991b.
- CONNORS, B. W. AND PRINCE, D. A. Effects of local anaesthetic QX-314 on the membrane properties of hippocampal pyramidal neurons. *J. Pharmacol. Exp. Ther.* 220: 476–481, 1982.
- DEKIN, M. S. AND GETTING, P. A. In vitro characterization of neurons in the ventral part of the nucleus tractus solitarius. II. Ionic basis for repetitive firing patterns. *J. Neurophysiol.* 58: 215–229, 1987.
- DI PASQUALE, E., TELL, F., MONTEAU, R., AND HILAIRE, G. Perinatal developmental changes in respiratory activity of medullary and spinal neurons: an in vitro study on fetal and newborn rats. *Dev. Brain Res.* 91: 121–130, 1996.
- FULTON, B. P. AND WALTON, K. Electrophysiological properties of neonatal rat motoneurons studied in vitro. *J. Physiol. (Lond.)* 370: 651–678, 1986.
- GETTING, P. A. Modification of neuron properties by electrotonic synapses I. Input resistance, time constant, and integration. *J. Neurophysiol.* 37: 846–857, 1974.
- GREER, J. J., SMITH, J. C., AND FELDMAN, J. L. Respiratory and locomotor patterns generated in the fetal rat brain stem-spinal cord in vitro. *J. Neurophysiol.* 67: 996–999, 1992.
- GU, X. AND SPITZER, N. C. Distinct aspects of neuronal differentiation encoded by frequency of spontaneous Ca^{2+} transients. *Nature* 375: 784–787, 1995.
- HARDING, R., HOOPER, S. B., AND VAN, V. K. Abolition of fetal breathing movements by spinal cord transection leads to reductions in fetal lung volume, lung growth and IGF-II gene expression. *Pediatr. Res.* 34: 148–153, 1993.
- HARRIS, A. J. AND MCCAIG, C. D. Motoneuron death and motor unit size during embryonic development of the rat. *J. Neurosci.* 4: 13–24, 1984.
- HILAIRE, G., KHATIB, M., AND MONTEAU, R. Central drive on Renshaw cells coupled with phrenic motoneurons. *Brain Res.* 376: 133–139, 1986.
- HOLLIDAY, J. AND SPITZER, N. C. Spontaneous calcium influx and its role in differentiation of spinal neurons in culture. *Dev. Biol.* 141: 13–23, 1990.
- JANSEN, A. H. AND CHERNICK, V. Fetal breathing and development of control of breathing. *J. Appl. Physiol.* 70: 1431–1446, 1991.
- JASSAR, B. S., PENNEFEATHER, P. S., AND SMITH, P. A. Changes in potassium channel activity following axotomy of B-cells in bullfrog sympathetic ganglion. *J. Physiol. (Lond.)* 497: 353–370, 1994.
- JIANG, C., AGULIAN, S., AND HADDAD, G. G. O_2 tension in adult and neonatal brain slices under several experimental conditions. *Brain Res.* 568: 159–164, 1991.
- KITTERMAN, J. A. The effects of mechanical forces on fetal lung growth. *Clin. Perinatol.* 23: 727–740, 1996.
- KOMURO, H. AND RAKIC, P. Intracellular Ca^{2+} fluctuations modulate the rate of neuronal migration. *Neuron* 17: 275–285, 1996.
- LANDMESSER, L. T. Growth cone guidance in the avian limb: a search for cellular and molecular mechanisms. In: *The Nerve Growth Cone*, edited by P. C. Letourneau, S. B. Kater, and E. R. Macagno, New York: Raven, 1992, p. 373–386.
- LIPSKI, J. Is there electrical coupling between phrenic motoneurons in cats? *Neurosci. Lett.* 46: 229–234, 1984.
- LOCKERY, S. R. AND SPITZER, N. C. Reconstruction of action potential development from whole-cell currents of differentiating spinal neurons. *J. Neurosci.* 12: 2268–2287, 1992.
- LOTURCO, J. L. AND KRIEGSTEIN, A. R. Clusters of coupled neuroblasts in embryonic neocortex. *Science* 252: 563–566, 1991.
- MARTIN-CARABALLO, M. AND GREER, J. J. Electrophysiological properties of phrenic motoneurons during fetal development. *XXXIII Int. Cong. Physiol. Sci. Abstr.*, P030, 1997a, p. 36.
- MARTIN-CARABALLO, M. AND GREER, J. J. Ionic mechanisms underlying changes in discharge properties of phrenic motoneurons during fetal development. *Soc. Neurosci. Abstr.* 635: 1997b.
- MCCOBB, D. P., BEST, P. M., AND BEAM, K. G. Development alters the expression of calcium currents in chick limb motoneurons. *Neuron* 2: 1633–1643, 1989.
- MCCOBB, D. P., BEST, P. M., AND BEAM, K. G. The differentiation of excitability on embryonic chick limb motoneurons. *J. Neurosci.* 10: 2974–2984, 1990.
- NORNES, H. O. AND DAS, G. D. Temporal pattern of neurogenesis in spinal cord of rat. I. An autoradiographic study—time and sites of origin and migration and settling patterns of neuroblasts. *Brain Res.* 73: 121–138, 1974.
- NUNEZ-ABADES, P. A., SPIELMANN, J. M., BARRIONUEVO, G., AND CAMERON, W. E. In vitro electrophysiology of developing genioglossal motoneurons in the rat. *J. Neurophysiol.* 70: 1401–1411, 1993.
- ONIMARU, H., BALLANYI, K., AND RICHTER, D. W. Calcium-dependent responses in neurons of the isolated respiratory network of newborn rats. *J. Physiol. (Lond.)* 491: 677–695, 1996.
- ROHRBOUGH, J. AND SPITZER, N. C. Regulation of intracellular Cl^- levels by Na^+ -dependent Cl^- cotransport distinguishes depolarizing from hyperpolarizing GABA_A receptor-mediated responses in spinal neurons. *J. Neurosci.* 16: 82–91, 1996.
- SPIGELMAN, I., ZHANG, L., AND CARLEN, P. L. Patch-clamp study of postnatal development of CA1 neurons in rat hippocampal slices: membrane excitability and K^+ currents. *J. Neurophysiol.* 68: 55–69, 1992.
- SPITZER, N. C. AND BACCAGLINI, P. I. Development of the action potential in embryonic amphibian neurons in vivo. *Brain Res.* 107: 610–616, 1976.

- TAKAHASHI, T. Membrane currents in visually identified motoneurons of neonatal rat spinal cord. *J. Physiol. (Lond.)* 423: 27–46, 1990.
- TORIKAI, H., HAYASHI, F., TANAKA, K., CHIBA, T., FUKUDA, Y., AND MIRIYA, H. Recruitment order and dendritic morphology of rat phrenic motoneurons. *J. Comp. Neurol.* 366: 231–243, 1996.
- VIANA, F., BAYLISS, D. A., AND BERGER, A. J. Calcium conductances and their role in the firing behaviour of neonatal rat hypoglossal motoneurons. *J. Neurophysiol.* 69: 2137–2149, 1993a.
- VIANA, F., BAYLISS, D. A., AND BERGER, A. J. Multiple potassium conductances and their role in action potential repolarization and repetitive firing behaviour of neonatal rat hypoglossal motoneurons. *J. Neurophysiol.* 69: 2150–2163, 1993b.
- VIANA, F., BAYLISS, D. A., AND BERGER, A. J. Postnatal changes in rat hypoglossal motoneuron membrane properties. *Neuroscience* 59: 131–148, 1994.
- WALTON, K. AND FULTON, B. P. Ionic mechanisms underlying the firing properties of rat neonatal motoneurons studied in vitro. *Neuroscience* 19: 669–683, 1986.
- WALTON, K. D. AND NAVARRETE, R. Postnatal changes in motoneuron electrotonic coupling studies in the in vitro rat lumbar spinal cord. *J. Physiol. (Lond.)* 43: 283–305, 1991.
- WU, W., ZISKIND-CONHAIM, L., AND SWEET, M. A. Early development of glycine- and GABA-mediated synapses in rat spinal cord. *J. Neurosci.* 12: 3935–3945, 1992.
- XIE, H. AND ZISKIND-CONHAIM, L. Blocking Ca^{2+} dependent synaptic release delays motoneuron differentiation in the rat spinal cord. *J. Neurosci.* 15: 5900–5911, 1995.
- ZISKIND-CONHAIM, L. Electrical properties of motoneurons in the spinal cord of the rat embryo. *Dev. Biol.* 128: 21–29, 1988.